Bioorganic & Medicinal Chemistry Letters 18 (2008) 5285–5289

Contents lists available at ScienceDirect

Bioorganic & Medicinal Chemistry Letters

journal homepage: www.elsevier.com/locate/bmcl

Kinase array design, back to front: Biaryl amides

Ian Baldwin, Paul Bamborough *, Claudine G. Haslam, Suchete S. Hunjan, Tim Longstaff, Christopher J. Mooney, Shila Patel †, Jo Quinn ‡, Don O. Somers

GlaxoSmithKline R&D, Medicines Research Centre, Gunnels Wood Road, Stevenage, Hertfordshire SG1 2NY, UK

ARTICLE INFO

Article history:
Received 25 July 2008
Revised 15 August 2008
Accepted 16 August 2008
Available online 22 August 2008

Keywords:
Kinase array design
p38 MAP kinase
p38a
cFMS
Inhibitors
Structure-based drug design

ABSTRACT

New kinase inhibitors can be found by synthesis of targeted arrays of compounds designed using system-based knowledge as well as through screening focused or diverse compounds. Most array strategies aim to add functionality to a fragment that binds in the purine subpocket of the ATP-site. Here, an alternative pharmacophore-guided array approach is described which set out to discover novel purine subpocket-binding groups. Results are shown for p38α and cFMS kinase, for which multiple distinct series with nanomolar potency were discovered. Some of the compounds showed potency in cell-based assays and good pharmacokinetic properties.

Most kinase inhibitors bind in the purine subpocket of the ATP-site using conserved H-bonding patterns to the 'hinge'. Typically, arrays designed to target kinases have used a single purine subpocket core, modified to extend into different parts of the ATP-site.[1] While often successful, such arrays only probe one purine subpocket group at a time. Here, we report a different approach to identify novel purine subpocket binders of kinases.

Some inhibitors interact with the lipophilic interior of the ATP-site (or 'back pocket') in kinases where this is accessible to gain potency and/or selectivity. Some of these, such as **1**, bind to the 'DFG-in' conformation of their targets, while others such as Gleevec, BIRB-796 and **2** bind in the DFG-out mode.[2,3] The back-pocket binding groups of these compounds make extensive interactions and contribute greatly to affinity. Here, we describe the use of these back-pocket binding groups as starting points from which to build out towards the front of the ATP-site. A similar 'back-to-front' approach was used to optimise the biaryl urea series to give BIRB-796.[2c] The work reported here differs in its intent, to identify new classes of kinase inhibitors for lead discovery as opposed to lead optimisation, and its use of arrays and pharmacophore-guided reagent selection together with multiple back-pocket groups utilising both DFG-in and DFG-out binding modes.

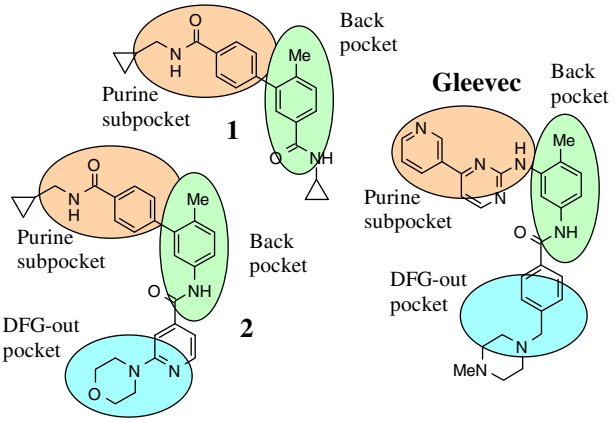

Crystal structures of **1** and **2** bound to p38α showed a critical hydrogen-bond from their cyclopropylmethyl amide carbonyls to the purine subpocket donor NH of Met109 (the 'hinge').[3] The short distance between this and the tolyl ring, together with the prevalence of aromatic rings in the purine pocket of kinase inhibitors, dictated the choice of chemistry used to build the arrays. Suzuki coupling allowed the insertion of a wide range of haloaryl rings targeting the purine subpocket.

* Corresponding author. Tel.: +44(0) 1438 763246; fax: +44(0) 1438 763352.
E-mail address: paul.a.bamborough@gsk.com (P. Bamborough).
† Present address: Biochemistry Department, Cambridge University, Tennis Court Road, Cambridge CB2 1GA, UK.
‡ Present address: Siena Biotech S.p.A., Strada del Petriccio e Belriguardo, 53100 Siena, Italy.

0960-894X/$ - see front matter © 2008 Elsevier Ltd. All rights reserved.
doi:10.1016/j.bmcl.2008.08.051

Back-pocket groups found in potent kinase inhibitors were chosen as starting points. **A–C** (Scheme 1) are substructures of potent biphenyl amide p38α inhibitors, such as **1** (K_i = 12 nM) and **2** (K_i = 4.4 nM).[3] **A** is found within compounds that bind in the DFG-in mode, while those containing **B** and **C** bind in the DFG-out mode. **D** is a fragment of Gleevec, a potent inhibitor of cAbl and other kinases including LCK and cFMS.[2a,4] Other fragments not included in this report were added to probe the back-pockets of other kinases.

Boronic acid esters **A–D** were prepared and coupled to a selection of aryl halides as shown in Scheme 1. Halides were chosen from a database of available reagents with the help of a pharmacophore model.[5] This defined the position of an aromatic ring on the tolyl ring together with a hydrogen-bond from the hinge Met109 NH. Coordinates were taken from the X-ray complex of **2** with p38α (Fig. 1).[3b]

The unreacted aryl bromides used to make compounds **3**, **6**, **8**, **14** and **19** all had K_i > 2μM against p38α, as did intermediate **F** (Scheme 1). However, the products of arrays **A–C** were expected to include potent p38α inhibitors. One hundred and seventy-two compounds from these arrays were successfully purified and were submitted for test against a panel of protein kinases. Table 1 shows the number of products from each array that were assayed. The 87 sub-100 nM compounds spanned 60 different purine subpocket-binding groups. Table 2 shows selected compounds and their p38α activities.

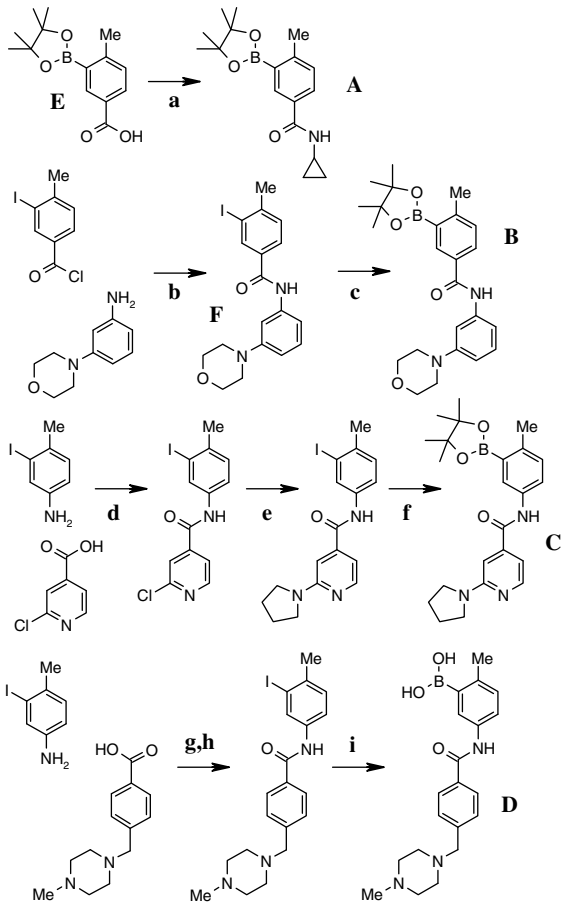

Scheme 1. Reagents and conditions: (a) cyclopropylamine, HATU, DIPEA, 3.5 h, rt; (b) DMF, Et_3N, 80 °C, 12 h; (c) bis(pinacolato)diborane, Et_3N, $PdCl_2$(dppf), dioxane, 80 °C, 12h; (d) HATU, DMF, DIPEA, 80 °C, 12 h; (e) pyrrolidine, 80 °C, 12 h; (f) bis(pinacolato)diborane, KOAc, $PdCl_2$(dppf), 80 °C, 12 h; (g) $SOCl_2$, $CHCl_3$, 80 °C, 16 h; (h) Et_3N, DMF, 50 °C, 16 h; (i) MeMgBr, sBuLi, $(EtO)_3B$, THF, −78 °C–rt, 16 h. **E** was prepared as previously described.[3a] **A–D** were coupled to aryl halides under Suzuki conditions using $Pd(PPh_3)_4$, Na_2CO_3 (aq), DME.

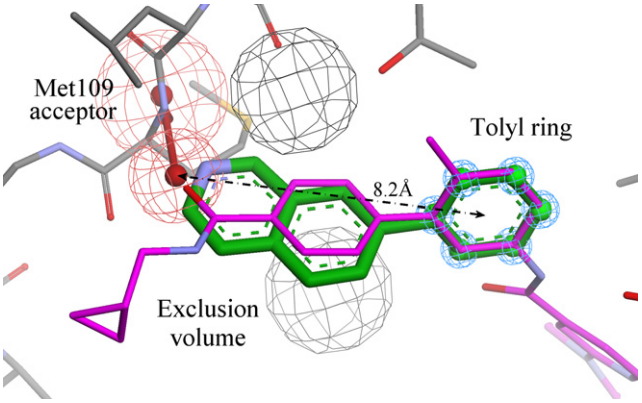

Figure 1. The pharmacophore search used to obtain the purine-site reagent list.[5] The p38α X-ray complex of **2** (magenta) defines the binding site. Pharmacophoric features (spheres) include the H-bond acceptor from Met109 NH (red, radius 1.25 and 1.75 Å for the projected point), tolyl ring aromatic atoms (blue, radii 0.5 Å) and excluded volumes (black, radii 1.7 Å). A representative isoquinoline hit that led to **14** is shown in green.

Table 1
Distribution of p38α compound activities by array[6]

Array	A	B	C	A–C	Purine pocket groups
Number tested	61	57	54	172	94
Number K_i <1 μM	47	50	49	146	84
Number K_i <100 nM	17	30	40	87	60
Number K_i <10 nM	4	6	7	17	12

X-ray structures of several examples have been solved in complex with p38α. Though alternative binding modes cannot be excluded for all compounds, especially the weaker inhibitors, the proposed back-pocket groups occupy the back-pocket of the site in all examples solved, and make the same extensive interactions as previously described for DFG-in and DFG-out binding biphenyl amides. [3]

Three types of p38α inhibitors will now be discussed. The first type includes aryl compounds *para*-substituted with a five-membered ring, for example the pyrazoles (**3c**), thiazoles (**4a–c**), and 1,2,4-oxadiazoles (**5a–c**).

Compounds from array A are generally less potent that those from arrays B and C. The 1,3,4-oxadiazoles (**6a–c**) are good examples of this type. A p38α X-ray structure was solved of the complex with **6a**.[7] It binds in the DFG-in mode in a similar way to **1**.[3a] The two structures are shown superimposed in Figure 2. As intended, the tolyl cyclopropylamide back-pocket group of **6a** mimics that of **1**. The amide group makes the same pair of hydrogen-bonds to Glu71 and Asp168 in the back-pocket. The oxadiazole ring occupies the purine subpocket and hydrogen-bonds to the hinge. One point of additional interest is that the hinge region of Gly110 flips, as previously reported for other structures, such that the backbone NH atoms of Met109 and Gly110 can both donate H-bonds to the oxadiazole nitrogens.[8]

It is interesting to compare **6a** to **20**, one of the first compounds from the biphenyl amide series (Fig. 3).[8] During the evolution of the series through several iterations, the oxadiazole in the back-pocket of **20** was first replaced by a cyclopropyl amide. Later, as described here, the purine-pocket amide was replaced by an oxadiazole. The location and substitution pattern of the central biphenyl group is maintained in both complexes, so this is not simply an example of a flipped binding mode.

Table 2
p38α activities (K_i, nM) of compounds from arrays **A–C** (Scheme 1)[6]

Purine-site group		Array			
		A	**B**	**C**	**D**
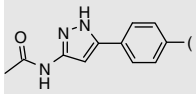	**3**			14	
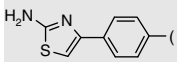	**4**	130	20	6.7	>850
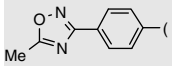	**5**	98	17	1.1	>850
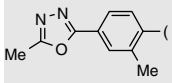	**6**	10	2.8	1.7	1400
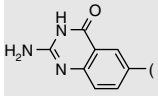	**7**	49	4.7	6.8	
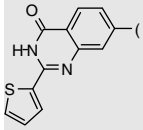	**8**	2.9			
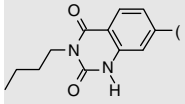	**9**	18	19	11	2000
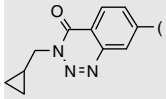	**10**	6			
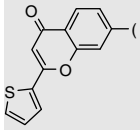	**11**	6.7			
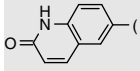	**12**		290	49	>2500
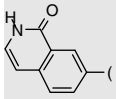	**13**	420	18	2.4	>2500
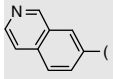	**14**	11	4.5		830
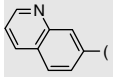	**15**	490			>2500
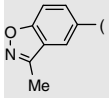	**16**	1100	380	160	

Table 2 (*continued*)

Purine-site group		Array			
		A	**B**	**C**	**D**
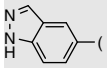	**17**	87	110		
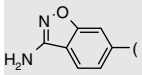	**18**	110	19	12	>850
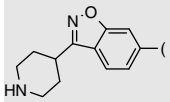	**19**	4	1.4	0.8	

Products that were impure or that gave inconsistent assay results are omitted, although some were later reprepared (data not shown).

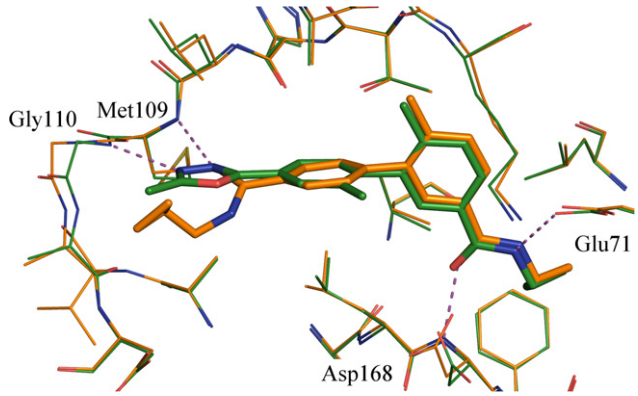

Figure 2. X-ray structure of **1** complexed with p38α (orange) superimposed on that of **6a** (green).

The second compound type contains fused 6,6-bicyclic systems. Some of these resemble cyclised biphenyl amides (for example **7–11**). These utilise the cyclic amide carbonyl oxygen to accept the hinge Met109 H-bond. The 6,6-bicyclic rings in which the cyclic amides are positioned at the 4-position to the biaryl linker have greater potency than those with the amide at the 3-position (compare **7a**–**8a**). This can be rationalised by their geometry being better able to H-bond to the hinge. Other 6,6-fused systems include those in which a ring nitrogen atom makes the hinge H-bond to Met109, for example, the isoquinolines **14a–b**. Once again, the importance of forming the hinge H-bond with appropriate geometry can be seen by comparing the potent isoquinoline **14a** to the less potent quinoline **15a**. While still fitting within the tolerances of the pharmacophore, the quinoline nitrogen of **15a** is not well placed to form the hinge H-bond. Similarly, compounds in which the hinge-binding nitrogen preferentially adopts the wrong tautomer are weaker (compare **14a**–**13a**, or **14b**–**13b**).

The third compound type includes fused 5,6-bicyclic systems (**16–19**). Among the most potent are the benzimidazole **17a–b** and the benzisoxazoles **18a–c** and **19a–c**. In this class of compounds, additional bulk in the outer lipophilic pocket region is beneficial for activity (compare **19b** to **18b** or **19c** to **18c**). A crystal structure of the DFG-out binding benzisoxazole **19b** in complex with p38α was solved (Fig. 4).[7] The benzisoxazole nitrogen fulfils the intended role of hydrogen-bonding to the hinge of Met109. The back-pocket binding part of the structure resembles that of

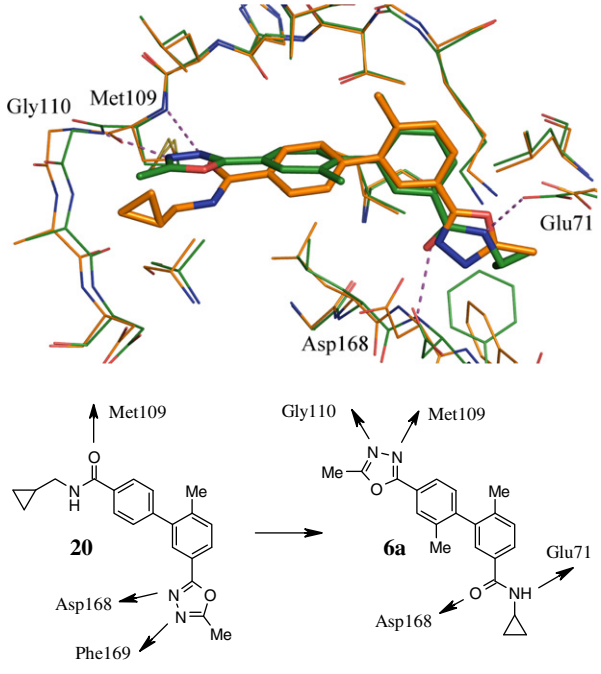

Figure 3. p38α crystal structures of **6a** (green) and **20** (orange).

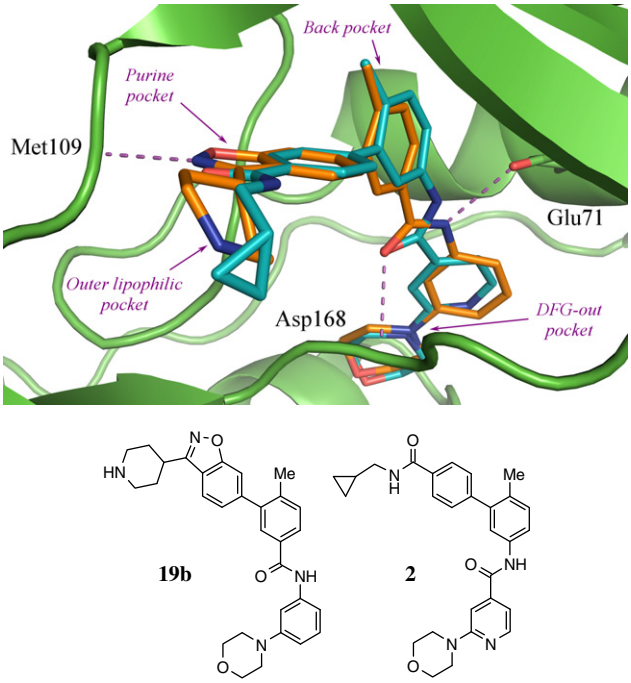

Figure 4. X-ray complex of **19b** (orange/green ribbon) superimposed on **2** (cyan).

the biphenyl amide **2** previously reported (Fig. 4), even though the amide of **19b** is of reversed direction to that of **2**.[3b]

Selectivity profiles were assessed by screening against a panel of protein kinases. Compounds from the same arrays with the same back-pocket binding groups showed similar profiles (Table 3). Compounds binding to p38α in the DFG-out mode (arrays B and C) also showed activity in a cRaf/MEK/ERK cascade assay.[9] This was unsurprising, given the p38α activity of the DFG-out binding Raf inhibitor Sorafenib.[10] In contrast, compounds from array A were selective for p38α (Fig. 5).

Most other kinases tested were unaffected by compounds from arrays **A**–**C**. One exception was the isoquinoline **14a,** which showed sub-μM inhibition of VEGFR2 (KDR) (Table 3). No significant VEGFR2 activity was seen with other 6,6-fused bicyclic templates or with the other two substructural types reported here.

Compounds from array **D** showed a completely different inhibition profile (Tables 2 and 3). As expected, they did not inhibit p38α. Instead, as reported for Gleevec, members of this array inhibited cFMS and LCK.[2a,4] Compound **14d** showed the greatest inhibition of these two targets, with IC_{50} of 4 nM and 70 nM, respectively. Compound **14d** was less selective than other compounds from array **D** (also inhibiting EGFR and ErbB4). It is unclear why the quinolines **14a** and **14d** are both less selective than other compounds with the same back-pocket groups.

Selected compounds were evaluated for their ability to inhibit cytokine production in cells. Table 3 shows IC_{50} values for inhibition of TNFα production in peripheral blood mononuclear cells and in whole blood.[6] Several compounds, for example **6a**, **6c**, **10a** and **14a**, showed encouraging sub-micromolar activity, comparable to or better than that seen with **1**.[3a] Compound **6a** was submitted for pharmacokinetic analysis. Its rat PK profile was comparable to that of **1**, with low plasma clearance, moderate volume of distribution and good bioavailability, but with a longer half-life (Table 4).[3a,11]

In summary, a pharmacophore-guided array strategy has been exploited to combine DFG-in and DFG-out back-pocket binding groups with novel kinase purine subpocket binders. The example of p38α has been used to illustrate the approach. Inhibitors with excellent enzyme potency and selectivity were produced without additional iterations of optimisation. The strategy has been validated by crystallographic confirmation of the intended binding mode. Multiple diverse and novel series were identified as promising p38α backup series to the biphenyl amides. Some of these also

Table 3
Kinase selectivity profiles and inhibition of TNFα production in PBMC cells and whole blood (IC_{50} μM)[6]

Compound	Array	Purine-site	Raf/Mek/Erk	CDK2	cFMS	EGFR	ErbB4	JNK3	LCK	PLK1	SGK1	VEGFR2	PBMC	HWB
19b	B	Benzisoxazole	0.04	>20	>20	>25	>25	>16	8	>25	>33	>20		
6b	B	1,3,4-Oxadiazole	0.4	>20	0.7	>25	>25	>16	8	>25	>33	6		
19c	C	Benzisoxazole	0.03	>20	7	>25	>25	>16	6	>25	>33	>20	0.06	5
6c	C	1,3,4-Oxadiazole	0.2	>20	>20	>25	>25	>16	10	>25	>33	>20	0.1	0.7
19a	A	Benzisoxazole	>50	>20	>20	>25	>25	>16	>16	>25	>33	>20	0.2	3
6a	A	1,3,4-Oxadiazole	20	>20	>20	>25	>25	>16	>16	>25	>33	>20	0.1	1
10a	A	1,2,3-Benzotriazinone		>20	>20	>25	>25	>16	>16	>25	32	>20	0.4	0.5
14a	A	Isoquinoline		>20	0.6	>25	>25	>16	3	>25	>33	0.5	0.1	0.1
1	A	Biphenylamide	>50	>20	>20	>25	>25	>16	>16	>25	>33	>20	0.25	1
6d	D	1,3,4-Oxadiazole		>20	0.1	>25	>25	>16	3	>25	>33	>20		
14d	D	Isoquinoline		>20	0.004	0.7	0.3	>16	0.07	>25	>33	0.80		
18d	D	Benzisoxazole		>20	0.09	>25	>25	>16	1	>25	>33	>20		
4d	D	Thiazole		>20	0.09	>25	>25	>16	2	>25	>33	>20		

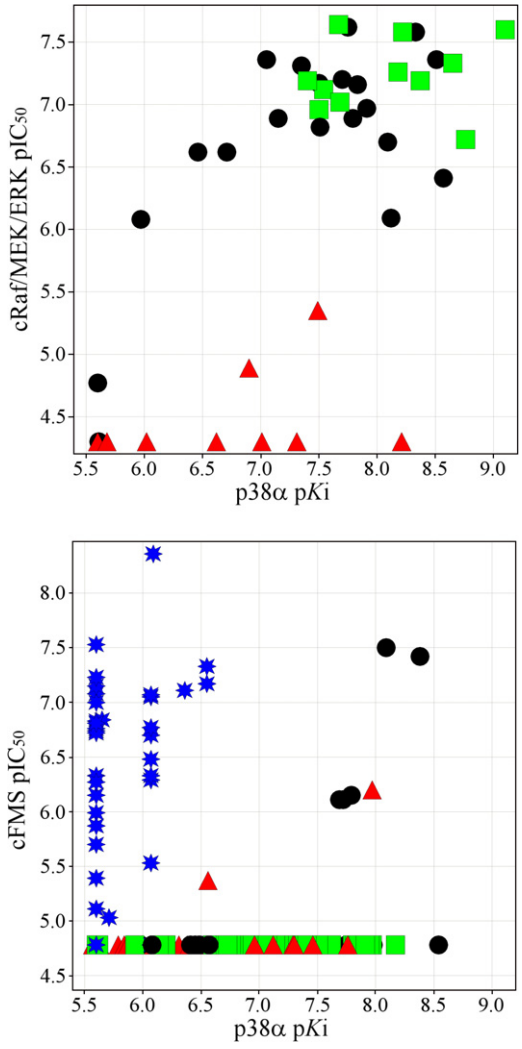

Figure. 5. *Top:* Plot of p38α against cRaf/MEK/ERK activity showing the greater selectivity of DFG-in compounds (array A, red diamonds) compared to DFG-out (array B, black circles, array C, green squares). *Bottom:* p38α against cFMS activity, showing the greater cFMS activity of array D (blue stars).

Table 4
Pharmacokinetic parameters of **6a** measured in rat[11]

IV plasma clearance (mL/min/kg)	3
IV steady state volume of distribution (L/kg)	1.2
IV plasma terminal $t_{1/2}$ (h)	4.6
PO $AUC_{(0-12\ h)}$ (ng h/mL)	4180
PO bioavailability	91%

showed favourable cellular activity and oral pharmacokinetic properties. Further development of these series will be described in future publications.

Acknowledgments

The authors thank Tony Angell for generating cellular data and Chun-wa Chung, Chris Edwards, Katherine Jones, Vipul Patel and Ann Walker for critical reading of the manuscript.

References and notes

1. (a) Lai, J.; Langston, S.; Adams, R.; Beevers, R.; Boyce, R.; Burckhardt, S.; Cobb, J.; Ferguson, Y.; Figueroa, E.; Grimster, N.; Henry, A.; Khan, N.; Jenkins, K.; Jones, M.; Judkins, R.; Major, J.; Masood, A.; Nally, J.; Payne, H.; Payne, L.; Raphy, G.; Raynham, T.; Reader, J.; Reader, V.; Reid, A.; Ruprah, P.; Shaw, M.; Sore, H.; Stirling, M.; Talbot, A.; Taylor, J.; Thompson, S.; Wada, H.; Walker, D. *Med. Res. Rev.* **2005**, *25*, 310; (b) Birault, V.; Harris, J.; Le, J.; Lipkin, M.; Nerella, R.; Stevens, A. *Curr. Med. Chem.* **2006**, *13*, 1735; (c) Prien, O. *ChemBioChem* **2005**, *6*, 500.
2. (a) Schindler, T.; Bornmann, W.; Pellicena, P.; Miller, W.; Clarkson, B.; Kuriyan, J. *Science* **2000**, *289*, 1938; (b) Pargellis, C.; Tong, L.; Churchill, L.; Cirillo, P.; Gilmore, T.; Graham, A.; Grob, P.; Hickey, E.; Moss, N.; Pav, S.; Regan, J. *Nat. Struct. Biol.* **2002**, *9*, 268; (c) Regan, J.; Breitfelder, S.; Cirillo, P.; Gilmore, T.; Graham, A.; Hickey, E.; Klaus, B.; Madwed, J.; Moriak, M.; Moss, N.; Pargellis, C.; Pav, S.; Proto, A.; Swinamer, A.; Tong, L.; Torcellini, C. *J. Med. Chem.* **2002**, *45*, 2994.
3. (a) Angell, R.; Aston, N.; Bamborough, P.; Buckton, J.; Cockerill, S.; deBoeck, S.; Edwards, C.; Holmes, D.; Jones, K.; Laine, D.; Patel, S.; Smee, P.; Smith, K.; Somers, D.; Walker, A. *Bioorg. Med. Chem. Lett.* **2008**, *15*, 4428; (b) Angell, R.; Angell, T.; Bamborough, P.; Bamford, M.; Chung, C.; Cockerill, S.; Flack, S.; Jones, K.; Laine, D.; Longstaff, T.; Ludbrook, S.; Pearson, R.; Smith, K.; Smee, P.; Somers, D.; Walker, A. *Bioorg. Med. Chem. Lett.* **2008**, *15*, 4433.
4. (a) Jacobs, M. D.; Caron, P. R.; Hare, B. J. *Proteins* **2008**, *70*, 1451; (b) b) Dewar, A. L.; Cambareri, A. C.; Zannettino, C. W.; Miller, B. L.; Doherty, K. V.; Hughes, T. P.; Lyons, A. B. *Blood* **2005**, *105*, 3127.
5. A sub-set of a small-molecule X-ray crystal structure database (Allen, F.; *Acta Cryst*., **2002**, *B58*, 380) was converted into Catalyst format (Accelrys Inc.) and searched using a 3D pharmacophore query built using the X-ray complex of **2** in p38α. Molecules hitting the query were processed to retain only the subgraphs containing the query features. These were converted into a 2D SMARTS representation (Daylight Chemical Systems Inc.) with generic atoms and bonds, with the exception of the hinge H-bond acceptor atom and an attachment Br or I atom replacing the tolyl ring of the query. The SMARTS queries were then used to search the GSK database for available reagents, which were examined and filtered by eye.
6. p38α K_i determinations, detecting displacement of a fluorescent ATP-competitive inhibitor, and IC_{50} values for inhibition of TNFα release from LPS-stimulated peripheral blood mononuclear cells (PBMCs) were carried out as described in Angell, R. et al. *Bioorg. Med. Chem. Lett*. **2008**, *18*, 324. Inhibition of TNFα release from whole blood cells was carried out as described[3a].
7. Unphosphorylated p38α was expressed, purified and crystallized as previously described (Angell, R. et al. *Bioorg. Med. Chem. Lett.* **2008**, *18*, 318). *Apo*-crystals were soaked with **6a** at 0.25 mM for 3 days or **19b** at 0.1 mM for 1 day. Both were cryoprotected for data collection at 100 K using an Oxford Cryostream. X-ray diffraction data were collected and processed and the structures solved as previously described.[3a] The final R-factor achieved for each complex was 17.2% for compound **6a** and 16.9% for compound **19b**. The coordinates have been deposited in the PDB as entries 3E92 and 3E93. Figures were produced using Pymol (DeLano, W.L., DeLano Scientific, Palo Alto CA, USA. http://www.pymol.org).
8. Angell, R.; Bamborough, P.; Cleasby, A.; Cockerill, S.; Jones, K.; Mooney, C.; Neu, M.; Somers, D.; Walker, A. *Bioorg. Med. Chem. Lett.* **2008**, *18*, 318. and references therein.
9. McDonald, O. B.; Chen, W.; Ellis, B.; Hoffman, C.; Overton, L.; Rink, M.; Smith, A.; Marshalland, C.; Wood, E. *Anal. Biochem.* **1999**, *268*, 318.
10. Wilhelm, S.; Carter, C.; Lynch, M.; Lowinger, T.; Dumas, J.; Smith, R.; Schwartz, B.; Simantov, R.; Kelley, S. *Nat. Rev. Drug Discov.* **2006**, *5*, 835.
11. Pharmacokinetic parameters derived from a composite blood sampling profile in male Lewis rats were determined following intravenous (iv) and oral (po) administration at 1 mg/kg. Compound was administered as a solution in 10% DMSO/70% PEG200/20% water. Blood was collected over a 12 h time period. Plasma preparation, sample analysis and data generation were carried out as described in Ref. 3a.